

DOI: 10.1002/cssc.201200242

Electron-Rich Anthracene Semiconductors Containing Triarylamine for Solution-Processed Small-Molecule Organic Solar Cells

Hyeju Choi,^[a] Hye Min Ko,^[a] Nara Cho,^[a] Kihyung Song,^[c] Jae Kwan Lee,^{*,[b]} and Jaejung Ko^{*,[a]}

New electron-rich anthracene derivatives containing triarylamine hole stabilizers, 2,6-bis[5,5'-bis(*N,N'*-diphenylaniline)-2,2'-bithiophen-5-yl]-9,10-bis-[(triisopropylsilyl)ethynyl]anthracene (TIPSAntBT-TPA) and 2,6-bis(5,5'-bis[4-[bis(9,9-dimethyl-9*H*-fluoren-2-yl)amino]phenyl]-2,2'-bithiophen-5-yl)-9,10-bis-[(triisopropylsilyl)ethynyl]anthracene (TIPSAntBT-bisDMFA), linked with π -conjugated bithiophene bridges, were synthesized and their photovoltaic characteristics were investigated in solution-processed small-molecule organic solar cells (SMOSCs). These new

materials exhibited superior intramolecular charge transfer from triarylamine to anthracene, leading to a more electron-rich anthracene core that facilitated electron transfer into phenyl- C_{61} -butyric acid methyl ester. Compared with TIPSAntBT and triarylamine, these materials show a threefold improvement in hole-transporting properties and better photovoltaic performance in solution-processed SMOSCs, with the best power conversion efficiency being 2.96% at a high open-circuit voltage of 0.85 V.

Introduction

Solution-processed organic solar cells (OSCs) fabricated by means of versatile printing techniques, such as doctor blade, inkjet, and roll-to-roll, offer a range of benefits that include low cost and light weights. In recent years, efforts have focused on improving device performance with the aim of achieving a power conversion efficiency (PCE) of 10%. New photoactive materials, such as π -conjugated (semiconducting) polymers and fullerene derivatives, have been developed in combination with functional layers that provide buffering, charge transport, and optical spacing.^[1] Recently, OSCs that promise PCEs above 8% have become strong candidates for the next generation of solar cells, threatening to replace inorganic thin-film and dye-sensitized solar cells (DSSCs).^[2] The highest efficiencies have been reported for OSCs fabricated with bulk-heterojunction (BHJ) materials comprised of low band gap semiconducting polymers and [6,6]-phenyl- C_{61} (or γ_1)-butyric acid methyl ester (PC₆₁(or γ_1)BM).^[3] However, these polymers suffer from the disadvantages of low reproducibility of certain characteristics (for example, weight-average molecular weight and polydispersity index) and difficulties in purification. Thus, small-molecule organic semiconductors appear to be more attractive from the viewpoint of mass production for commercial applications, and considerable research effort has been focused on developing efficient small-molecule materials for improved device performance, with the short-term goal being a PCE comparable to that of polymer-based solar cells.^[4] Indeed, recent breakthroughs in realizing PCEs of above 6% have placed solution-processed small-molecule organic solar cells (SMOSCs) squarely in competition with polymer-based cells.^[5]

Efficient organic semiconductors used in SMOSCs often have structural core motifs,^[4] such as oligothiophene, bridged dithiophene, benzothiadiazole, squaraine, or diketopyrrolopyr-

role, inspired by low band gap semiconducting polymers or push-pull molecular structures in nonlinear optics and DSSCs because of their superior optoelectronic properties. Recently, we also reported various symmetric or asymmetric push-pull chromophores for solution-processed SMOSCs.^[6] These push-pull structures in SMOSCs enable efficient intramolecular charge transfer (ICT), giving the chromophore better molar absorptivity. In addition, an electron-donating group, such as triphenylamine (TPA), can play an important role in stabilizing holes separate from excitons and improving the transporting property of the hole carrier.^[4,6]

However, these small molecules have often exhibited poor molecular packing and intermolecular interactions in spin-cast BHJ composite films with PC₇₁BM, resulting in low charge-carrier mobility. Therefore, we became interested in solution processable and highly crystallizable small molecules, such as pentacene and anthracene derivatives, as an efficient core motif

[a] H. Choi, H. M. Ko, N. Cho, Prof. J. Ko
Department of New Materials Chemistry
Korea University, Chungnam, 330-700 (South Korea)
Fax: (+82) 44-860-1331
E-mail: jko@korea.ac.kr

[b] Prof. J. K. Lee
Department of Chemistry Education
Chosun University, Gwangju, 501-759 (South Korea)
Fax: (+82) 62-230-7319
E-mail: chemedujk@chosun.ac.kr

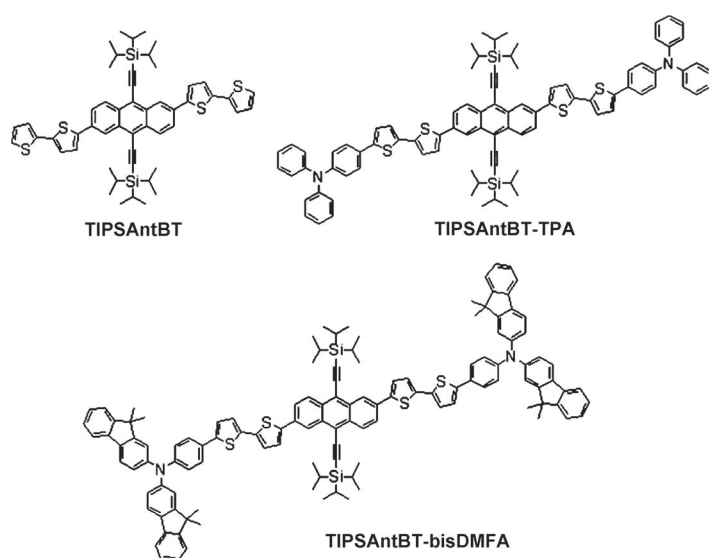
[c] Prof. K. Song
Department of Chemical Education
Korea National University of Education
Chungbuk, 333-791 (South Korea)

Supporting Information for this article is available on the WWW under <http://dx.doi.org/10.1002/cssc.201200242>.

for organic semiconductors in SMOSCs.^[7] These small-molecule semiconductors show excellent electron- and hole-transporting properties, with field-effect mobilities over $1 \text{ cm}^2 \text{ V}^{-1} \text{ s}$.^[8] In this study, we tried to develop new small-molecule organic semiconductors based on the soluble and crystallizable anthracene derivative 6,13-bis(triisopropylsilyl)ethynylanthracene (TIPSAnt) for solution-processed SMOSCs. Recently, Chung et al. reported an SMOSC with a PCE of 1.4%, with bithiophene substituted for the TIPSAnt derivative and a PC₇₁BM BHJ-active layer.^[9] Although the single crystalline structure showed a high mobility of $0.2 \text{ cm}^2 \text{ V}^{-1} \text{ s}$ in a field-effect transistor device,^[8] the low PCE in the SMOSC was mainly the result of a low photocurrent. This could be due to it having insufficient structural strength to stabilize the excitons conducted by absorbed light in the BHJ-active layer with PC₇₁BM, as well as its low molar absorptivity.

Herein, we report the synthesis and photovoltaic characteristics of new electron-rich anthracene derivatives containing triarylamine hole stabilizers, 2,6-bis[5,5'-bis(*N,N'*-diphenylamino)-2,2'-bithiophen-5-yl]-9,10-bis-[(triisopropylsilyl)ethynyl]anthracene (TIPSAntBT-TPA) and 2,6-bis(5,5'-bis[4-[bis(9,9-dimethyl-9*H*-fluoren-2-yl)amino]phenyl]-2,2'-bithiophen-5-yl)-9,10-bis-[(triisopropylsilyl)ethynyl]anthracene (TIPSAntBT-bisDMFA), for use as efficient solution-processed SMOSCs. These semiconductors were compared with the 2,6-di(2'-bithiophen-5-yl)-9,10-bis-[(triisopropylsilyl)ethynyl]anthracene (TIPSAntBT) devices reported previously and had a PCE of 2.96% with a high open-circuit voltage of 0.85 V (Scheme 1).

In addition, two triarylamines of TPA and bisDMFA were compared to investigate their role as electron donors and hole stabilizers. Both of these newly synthesized materials, TIPSAntBT-TPA and TIPSAntBT-bisDMFA, presented superior ICT to anthracene through a π -conjugated bithiophene bridge, producing a more electron-rich anthracene core that could facilitate electron transfer into PC₇₁BM.



Scheme 1. Molecular structures of the anthracene derivatives containing triarylamine and the device architecture of a solution-processed SMOSC.

Results and Discussion

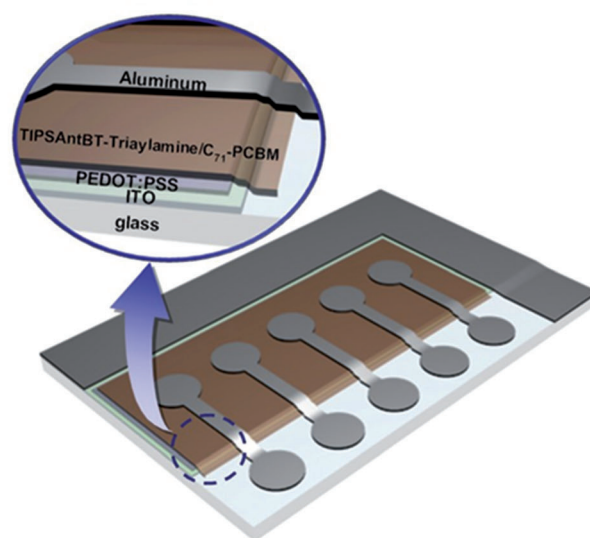
Synthesis and characterization

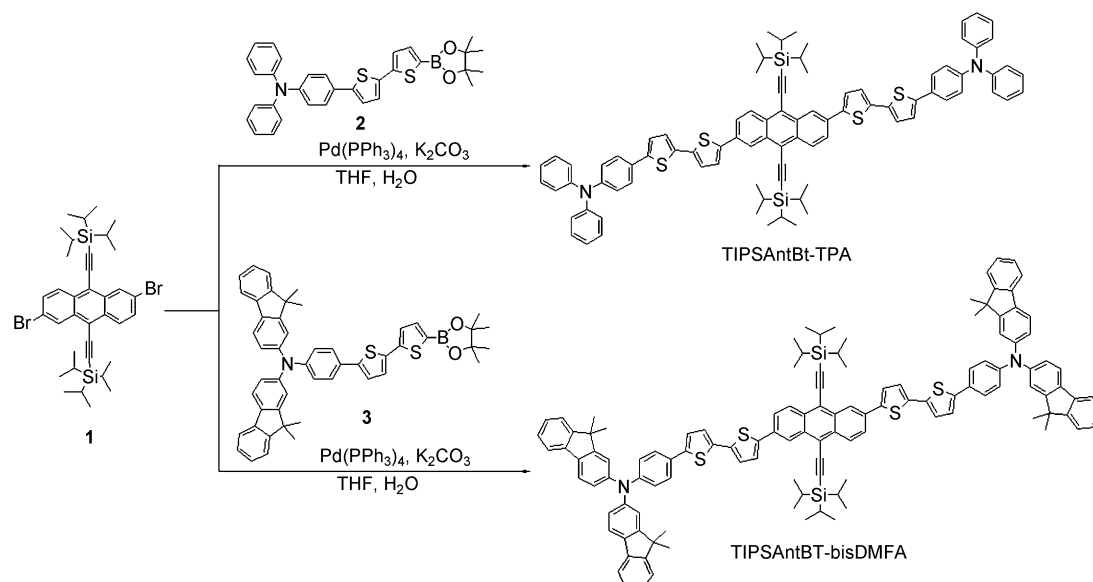
The synthetic methods used for the new semiconductors are outlined in Scheme 2. All reactions were carried out in a nitrogen atmosphere and 2,6-dibromo-9,10-bis[(triisopropylsilyl)ethynyl]anthracene (**1**), 5-bis(*N,N'*-diphenylamino)-2,2'-bithiophene, and 5-bis[4-[bis(9,9-dimethyl-9*H*-fluoren-2-yl)amino]phenyl]-2,2'-bithiophene were readily synthesized, according to a procedure reported previously.^[10]

The anthracene semiconductor TIPSAntBT-TPA was synthesized by using a stepwise synthetic protocol. Consecutive lithiation of 5-bis(*N,N'*-diphenylamino)-2,2'-bithiophene with *n*-butyllithium followed by the addition of 2-isopropoxy-4,4,5,5-tetramethyl-1,3,2-dioxaborolane successfully produced 5-bis(*N,N'*-diphenylamino)-5'-(4,4,5,5-tetramethyl-1,3,2-dioxaborolan-2-yl)-2,2'-bithiophene (**2**). Then, a Suzuki coupling reaction of **1** and **2** (1:2 molar ratio) successfully proceeded with moderate yield, leading to the final product, TIPSAntBT-TPA. TIPSAntBT-bisDMFA was synthesized by using the same synthetic procedure with compound **3** instead of **2**. The chemical structures of the synthesized products, TIPSAntBT-TPA and TIPSAntBT-bisDMFA, were verified by ¹H and ¹³C NMR spectroscopy and matrix-assisted laser desorption/ionization time of flight (MALDI-TOF) mass spectrometry. These materials have good solubility in common organic solvents, such as dichloromethane, chloroform, chlorobenzene, and toluene. These details are described further in the Supporting Information.

Optical properties and time-dependent DFT calculations

Figure 1 shows the UV/Vis absorption spectra of TIPSAntBT, TIPSAntBT-TPA, and TIPSAntBT-bisDMFA in chlorobenzene and as thin films. The corresponding optical properties are summarized in Table 1.





Scheme 2. Synthesis of the new organic semiconductors TIPSAntBT-TPA and TIPSAntBT-bisDMFA.

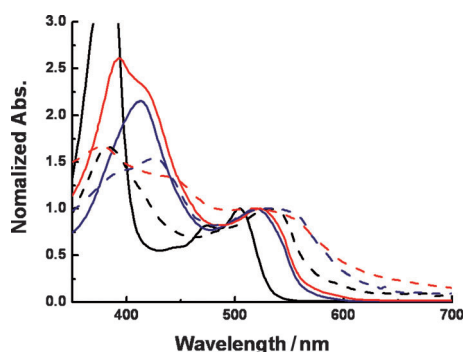


Figure 1. UV/Vis absorption spectra of TIPSAntBT (black), TIPSAntBT-TPA (blue), and TIPSAntBT-bisDMFA (red) in chlorobenzene (solid lines) and as thin films (dashed lines).

As shown in Figure 1, the transition absorption bands of TIPSAntBT (black), TIPSAntBT-TPA (blue), and TIPSAntBT-bisDMFA (red) in chlorobenzene (solid line) were observed in the wavelength region of 300–700 nm of the absorption spectra. Molecular calculations by time-dependent density function-

al theory (TD-DFT) using the B3LYP functional/6-31G* basis set might provide the information on these transition bands. Figure 2 shows the calculated energy levels of these materials in vacuo. The details are summarized in Table S1 in the Supporting Information. The absorption bands observed at a longer wavelength should result from ICT originating from HOMO→LUMO monoexcitations, as shown in Figure 2. Although TIPSAntBT was already reported by Chung et al.,^[9] there was little information about the four optical absorption transitions observed in the 300–700 nm region. These absorption peaks could be assigned to the π - π^* transition, which predominantly originate from HOMO→LUMO+1, HOMO-2→LUMO, and HOMO-1→LUMO transitions. The fourth peak, at a longer wavelength, should result from ICT between the bi-thiophene donor and the anthracene core.

On the other hand, TIPSAntBT-TPA and TIPSAntBT-bisDMFA modified with triarylamine exhibited redshifted absorption bands of 14 and 26 nm and molar absorptivities enhanced 3.2 and 3.6 times, respectively, relative to their unmodified counterpart, TIPSAntBT. Their ICT bands exhibited high molar absorption efficiencies ϵ of 45 626 mol⁻¹cm⁻¹ at 528 nm and 51 964 mol⁻¹cm⁻¹ at 530 nm, respectively. However, modification with triarylamine alone cannot significantly extend the π -conjugation length of TIPSAntBT. A redshift of the absorption spectrum and a high molar absorptivity are often observed in molecular structures with longer π conjugation. The broadened transition band of TIPSAntBT-TPA observed at 300–500 nm might overlap with the

Table 1. Optical and electrochemical properties of the TIPSAntBT-TPA and TIPSAntBT-bisDMFA.

Compounds	$\lambda_{\max}^{[a]}$ [nm] (ϵ [mol ⁻¹ cm ⁻¹])	$\lambda_{\max}^{[b]}$ [nm]	$E_{\text{onset, ox}}$ [V] /HOMO [eV] ^[c]	$E_{\text{onset, red}}$ [V] /LUMO [eV] ^[c]	ΔE_{onset} [eV] ^[d]	E_{onset} [eV] ^[e]
TIPSAntBT ^[h]	504 (14 370)	525	0.543/−5.343	1.590/−3.210	2.133	2.322
TIPSAntBT-TPA	528 (45 626)	532	0.222/−5.022	1.348/−3.452	1.570	2.202
TIPSAntBT-bisDMFA	530 (51 964)	532	0.411/−5.211	1.381/−3.419	1.792	2.189

[a] Absorption spectra were measured in chlorobenzene. [b] Absorption spectra were measured as solid-state thin films. [c] Energy levels were calculated from oxidation/reduction onsets of cyclic voltammogram (CV) spectra measured with a scan rate of 100 mV s⁻¹ in CH₂Cl₂ with 0.1 M (*n*-C₄H₉)₄NPF₆ using a ferrocenium/ferrocene (Fc) redox couple as an external reference. The HOMO and LUMO levels can be deduced from the oxidation and reduction onsets, under the assumption that the energy level of Fc versus a normal hydrogen electrode (NHE) is 4.8 eV below vacuum level. [d] ΔE_{onset} was calculated by LUMO−HOMO. [e] E_{onset} was determined from the onset of the absorption spectra. [g] These values were consistent with those reported in Ref. [9].

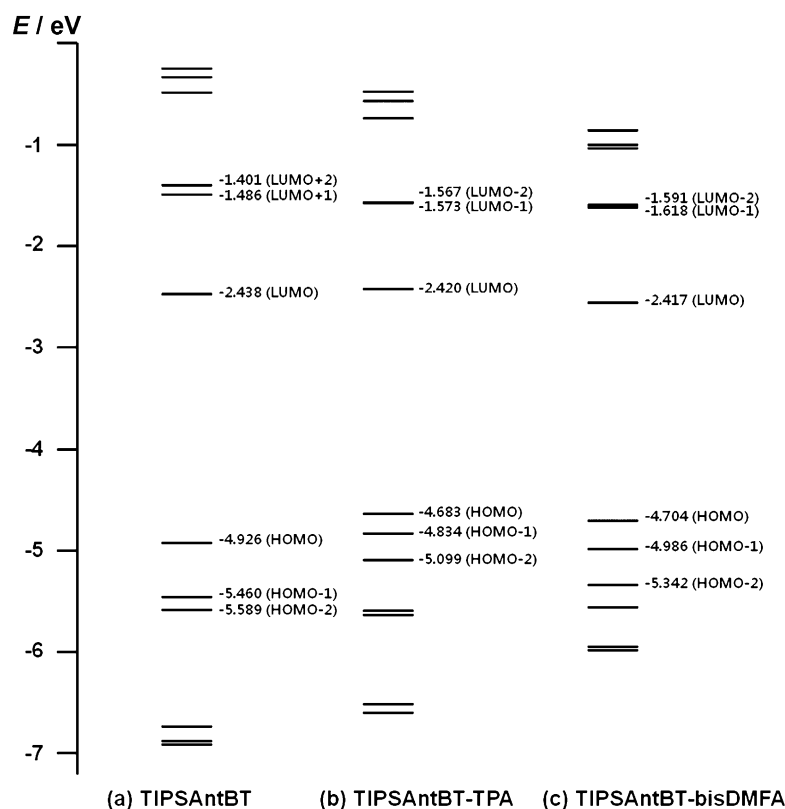


Figure 2. Orbital energies of a) TIPSAntBT, b) TIPSAntBT-TPA, and c) TIPSAntBT-bisDMFA calculated by TD-DFT using the B3LYP functional/6-31G* basis set.

transition bands of HOMO→LUMO+1 and HOMO−2→LUMO monoexcitations, whereas the transition at 450–600 nm seems to originate from HOMO→LUMO excitation ($f=1.044$) with minor HOMO−1→LUMO monoexcitations ($f=0.002$), showing very intense oscillator strengths (f) for the transitions. The absorption band of TIPSAntBT-bisDMFA exhibited similar transition characteristics (see the Table S1 in the Supporting Information). From these results, we note that the presence of more effective ICT from triarylamine to the anthracene core in TIPSAntBT-TPA and TIPSAntBT-bisDMFA leads to redshifted absorption and increased molar absorptivity, and bisDMFA shows a slightly better electron-donating capability than that of TPA.

To clarify the interpretation of these results, a molecular calculation analysis of TIPSAntBT, TIPSAntBT-TPA, and TIPSAntBT-bisDMFA was performed. Figure 3 shows the optimized structures of these materials calculated by means of TD-DFT using the B3LYP functional/6-31G* basis set. The orbital densities of the HOMO and LUMO of TIPSAntBT were observed for the π conjugation of anthracene–dithiophene and the anthracene core, respectively. The orbital density of the HOMO of TIPSAntBT-TPA (or bisDMFA) was evenly distributed on anthracene–dithiophene–TPA (or bisDMFA), but the orbital density of the LUMO of TIPSAntBT-TPA (or bisDMFA) was predominantly located on anthracene–dithiophene. This calculation reveals that the ICT from triarylamine to the anthracene core can occur effectively in TIPSAntBT-TPA and TIPSAntBT-bisDMFA

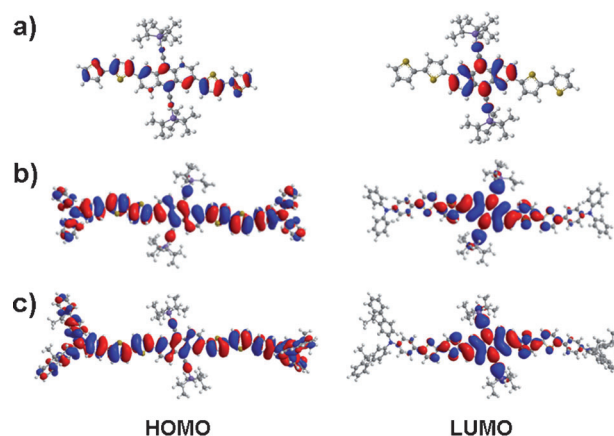


Figure 3. Isodensity surface plots of TIPSAntBT, TIPSAntBT-TPA, and TIPSAntBT-bisDMFA calculated by TD-DFT using the B3LYP functional/6-31G* basis set

fold higher hole mobility than that of TIPSAntBT. These results are discussed in detail below.

Electrochemical properties

Figure 4 shows cyclic voltammograms of TIPSAntBT, TIPSAntBT-TPA, and TIPSAntBT-bisDMFA in dichloromethane. The corresponding electrochemical properties are also summarized in Table 1. The energy levels of the HOMOs and

when excited by light energy, while TPA and bisDMFA can play a key role in stabilizing holes separate from excitons.

In a solid-state thin film, the absorption spectrum of TIPSAntBT (Figure 1, black dashed line) showed a π - π^* transition band redshifted by about 30 nm and a broader spectrum than that in solution, indicating that its flattened structure facilitated intermolecular packing interactions. However, an interesting finding was that films of TIPSAntBT-TPA (Figure 1, blue dashed line) and TIPSAntBT-bisDMFA (Figure 1, red dashed line) exhibited only broader spectra with slightly redshifted absorption bands. Amorphous nonplanar TPA and bisDMFA of TIPSAntBT-TPA and TIPSAntBT-bisDMFA might interrupt the intermolecular packing interactions in solid-state films. Nevertheless, TIPSAntBT-TPA (or bisDMFA) exhibited about three-

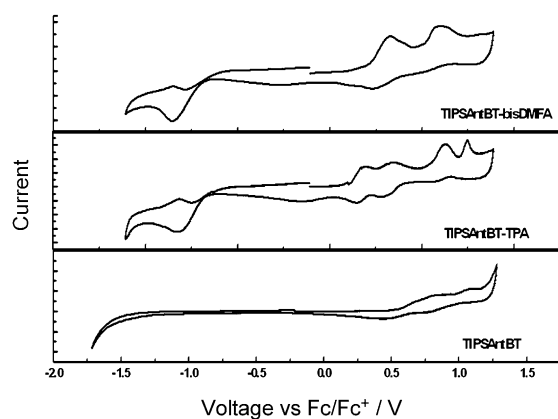


Figure 4. Electrochemical characterization of TIPSAntBT, TIPSAntBT-TPA, and TIPSAntBT-bisDMFA in dichloromethane/tetrabutylammonium hexafluorophosphate (TBAFP₆; 0.1 M) with a scan speed of 100 mV s⁻¹; potentials are given versus the external reference Fc/Fc⁺.

LUMOs of these materials were determined from these CV spectra. A platinum rod electrode, a platinum wire, and an Ag/AgNO₃ (0.10 M) electrode were used as the working electrode, counter electrode, and reference electrode, respectively. The analyses were performed in an electrolyte consisting of a 0.1 M solution of TBAFP₆ in dichloromethane at room temperature under nitrogen, with a scan rate of 100 mV s⁻¹, and an Fc/Fc⁺ redox couple was used as an external reference. The HOMO and LUMO levels can be deduced from the oxidation and reduction onsets, under the assumption that the energy level of Fc versus NHE^[11] is 4.8 eV below vacuum level. Cyclic voltammograms of these materials in solid-state thin films could not be recorded due to stripping of the film on the electrode. Therefore, we determined the optical band gap by calculating absorption thresholds from the absorption spectra of these materials in chlorobenzene.

The HOMO levels of TIPSAntBT, TIPSAntBT-TPA, and TIPSAntBT-bisDMFA, determined in solution by CV, were calculated to be 5.34, 5.02, and 5.21 eV, respectively. From these results, we can estimate that the V_{oc} of devices fabricated by using these materials and with PC₇₁BM BHJ-active layers could be in the range of 0.7–0.9 eV.^[12] Indeed, the V_{oc} values found in experiments were consistent with these expected values.

Photophysical properties

Figure 5a shows the UV-visible absorption spectra of the TIPSAntBT-TPA/PC₇₁BM (1:4; blue) and TIPSAntBT-bisDMFA/PC₇₁BM (1:4; red) films, which exhibited the best performances in a BHJ solar cell device. As shown in Figure 5a, the peaks in the absorption bands of TIPSAntBT-TPA (or bisDMFA) in the TIPSAntBT-TPA (or bisDMFA)/PC₇₁BM BHJ composites deposited from chlorobenzene were redshifted by about 20 nm relative to those of their pristine films, indicating interference in intermolecular π - π packing interactions by PC₇₁BM in the BHJ film.

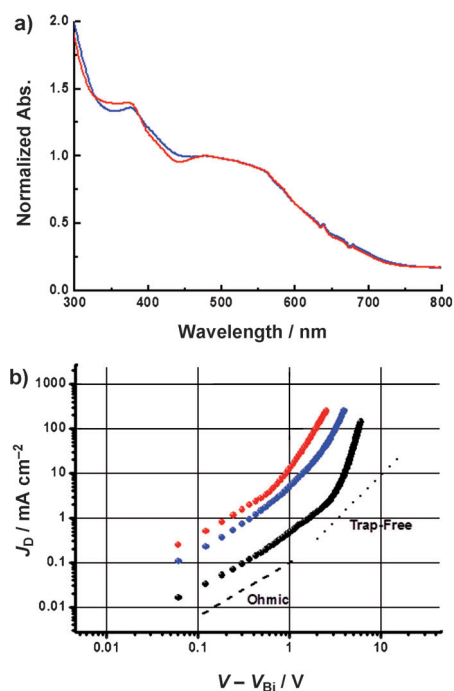


Figure 5. a) UV/vis absorption spectra and b) space-charge limitation of J - V characteristics of the TIPSAntBT-TPA/PC₇₁BM (1:4; blue) and TIPSAntBT-bisDMFA/PC₇₁BM (1:4; red) BHJ films, the hole-only devices of which (indium tin oxide (ITO)/poly(3,4-ethylenedioxythiophene):poly(styrenesulfonate) (PEDOT:PSS)/TIPSAntBT-TPA (or bisDMFA):PC₇₁BM/Au) were compared with those of TIPSAntBT/PC₇₁BM (1:1; black).

To investigate the space-charge effects, we extracted the hole mobilities of TIPSAntBT-TPA and TIPSAntBT-bisDMFA from the space-charge limitation of current (SCLC) J - V (current density-voltage) characteristics obtained in the dark for hole-only devices. The average hole mobilities were determined by measuring 20 cells, each of which was measured three times to compensate for errors in measurement. Compared with TIPSAntBT, TIPSAntBT-TPA and TIPSAntBT-bisDMFA showed improved efficiency at an 1:4 ratio with PC₇₁BM, giving results similar to those reported by Chung et al.^[9] Figure 5b shows the dark-current characteristics of ITO/PEDOT:PSS/Donor:PC₇₁BM/Au devices as a function of the bias, corrected by the built-in voltage determined from the difference in work function between Au and the HOMO level of TIPSAntBT-TPA (or bisDMFA). Ohm's law can be observed at low voltages as an effect of thermal-free carriers. For the presence of carrier traps in the active layer, there is a trap-filled-limit (TFL) region between the ohmic and the trap-free SCLC regions. The SCLC behavior in the trap-free region can be characterized by using the Mott-Gurney square law [Eq. (1)].^[13]

$$J = (9/8)\epsilon\mu(V^2/L^3) \quad (1)$$

in which ϵ is the static dielectric constant of the medium and μ is the carrier mobility.

The hole mobilities of TIPSAntBT, TIPSAntBT-TPA, and TIPSAntBT-bisDMFA, as evaluated by using Equation (1) ($\epsilon = 3\epsilon_0$), were 3.32×10^{-6} , 1.02×10^{-5} , and 1.12×10^{-5} cm² V⁻¹ s⁻¹, re-

spectively. Although strong intermolecular packing interactions of anthracene, for high hole mobility, was significantly interrupted by amorphous nonplanar triarylamine, as shown in Figure 5, the hole mobilities of TIPSAntBT-TPA and TIPSAntBT-bisDMFA were about three times higher than that of flattened TIPSAntBT without triarylamine. These results indicate that the triarylamine group of TIPSAntBT-TPA (or bisDMFA) can effectively stabilize the hole separated from the exciton in the BHJ system with PC₇₁BM to reduce charge recombination between the donor and PC₇₁BM, leading to an increase in the transporting properties of the hole carrier.

Photovoltaic performances

The performances of TIPSAntBT-TPA and TIPSAntBT-bisDMFA were investigated through the application of a photovoltaic device fabricated with these materials on PC₇₁BM BHJ films. A study of the characteristics of over 300 solar cells revealed that the most efficient photovoltaic cells were those obtained from a BHJ system of TIPSAntBT-TPA (or TIPSAntBT-bisDMFA) with PC₇₁BM, which were optimized at a ratio of approximately 1:4. These BHJ films were cast on top of a PEDOT:PSS (Heraeus, AI 4083) layer. The optimum thicknesses of the TIPSAntBT-TPA/PC₇₁BM and TIPSAntBT-bisDMFA/PC₇₁BM BHJ films obtained under these conditions were around 64 and 86 nm, respectively.

Figure 6 shows the J - V curves under AM 1.5 illumination conditions (100 mW cm^{-2}) and the incident-photon-to-current efficiency (IPCE) spectra of TIPSAntBT-TPA (or bisDMFA)/PC₇₁BM BHJ solar cells fabricated under optimized processing conditions, with 1-chloronaphtalene (CN) as the processing additive^[6a] (or TiO_x, which can effectively act as an optical spacer and buffer layer^[14]). The corresponding values are summarized in Table 2. The IPCE spectra of these devices, as shown in Figure 6b, exhibit curves that are well matched with their photocurrents in the J - V curves.

Donor	Treatment	J_{sc} [mA cm ⁻²]	V_{oc} [V]	FF [%]	Efficiency [%]
TIPSAntBT ^[b]	none	4.25	0.85	38	1.38
TIPSAntBT-TPA	none	4.57	0.53	33	0.81
TIPSAntBT-TPA	1% CN	5.19	0.56	32	0.95
TIPSAntBT-TPA	1% CN, TiO _x	6.07	0.72	40	1.97
TIPSAntBT-bisDMFA	none	4.92	0.59	33	0.96
TIPSAntBT-bisDMFA	1% CN	6.80	0.77	36	1.90
TIPSAntBT-bisDMFA	1% CN, TiO _x	8.58	0.85	41	2.96

[a] The optimum devices were fabricated with TIPSAntBT/PC₇₁BM (1:1), TIPSAntBT-TPA/PC₇₁BM (1:4), and TIPSAntBT-bisDMFA/PC₇₁BM (1:4). Performances were determined under simulated 100 mW cm^{-2} AM 1.5G illumination. The light intensity was set by using calibrated standard silicon solar cells with a proactive window made from KG5 filter glass from the National Renewable Energy Laboratory (NREL). The masked active area of the device was 4 mm^2 . [b] These values were similar to those reported in Ref. [9].

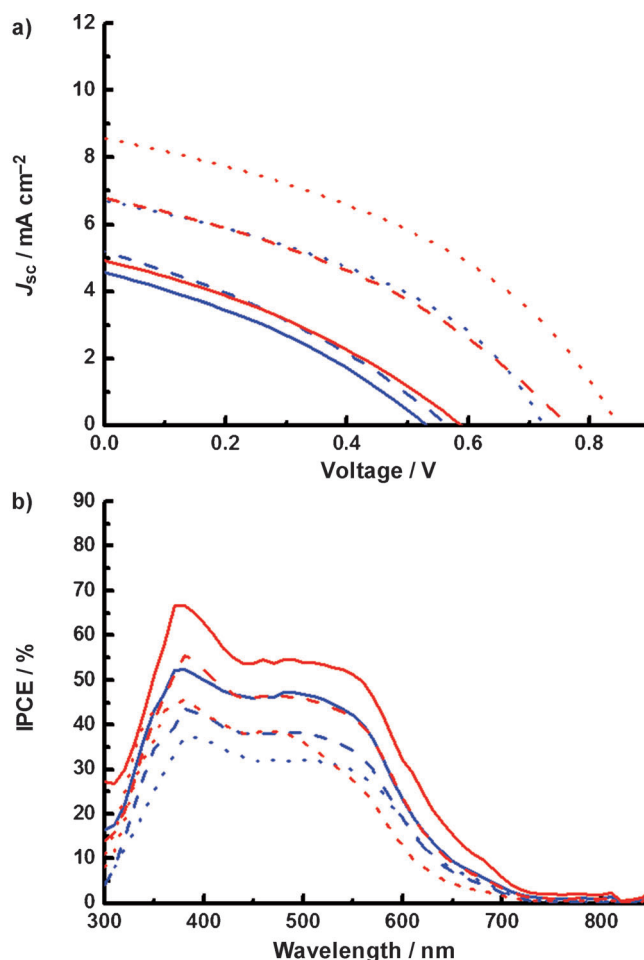


Figure 6. J - V curves (a) under AM 1.5 conditions (100 mW cm^{-2}) and IPCE spectra (b) of TIPSAntBT-TPA (blue) or TIPSAntBT-bisDMFA (red)/PC₇₁BM BHJ solar cells fabricated under optimized processing conditions with 1% CN processing additive with (—)/without (---) insertion of a TiO_x layer or without additive and TiO_x layer (.....).

As shown in Figure 6 and Table 2, the devices conventionally fabricated with TIPSAntBT-bisDMFA/PC₇₁BM and TIPSAntBT-TPA/PC₇₁BM exhibited a PCE of 0.96% (± 0.12) with a short-circuit current density (J_{sc}) of 4.92 mA cm^{-2} , a fill factor (FF) of 0.33, and an open-circuit voltage (V_{oc}) of 0.59 V, and a PCE of 0.81% (± 0.11) with $J_{sc} = 4.57 \text{ mA cm}^{-2}$, $FF = 0.33$, and $V_{oc} = 0.53 \text{ V}$, respectively. These values indicate an efficiency reduced by 30–40% compared with that of TIPSAntBT without triarylamine. This could be due to the inferior BHJ morphologies of TIPSAntBT-bisDMFA/PC₇₁BM and TIPSAntBT-TPA/PC₇₁BM, as shown in Figure 7. The processing additive approach with CN clearly improved the performance of the devices because the processing additive delivered better morphologies of TIPSAntBT-bisDMFA/PC₇₁BM and TIPSAntBT-TPA/PC₇₁BM BHJ film.^[6a, 14]

In addition, the insertion of a TiO_x layer often allowed the device to increase light absorption and improved contact between the active layer and the metal electrode.^[13] Therefore, we obtained the best PCE of 2.96% (± 0.2) in devices fabricated with a TIPSAntBT-bisDMFA/PC₇₁BM film treated with a CN processing additive and a TiO_x layer: $J_{sc} = 8.58 \text{ mA cm}^{-2}$, $FF =$

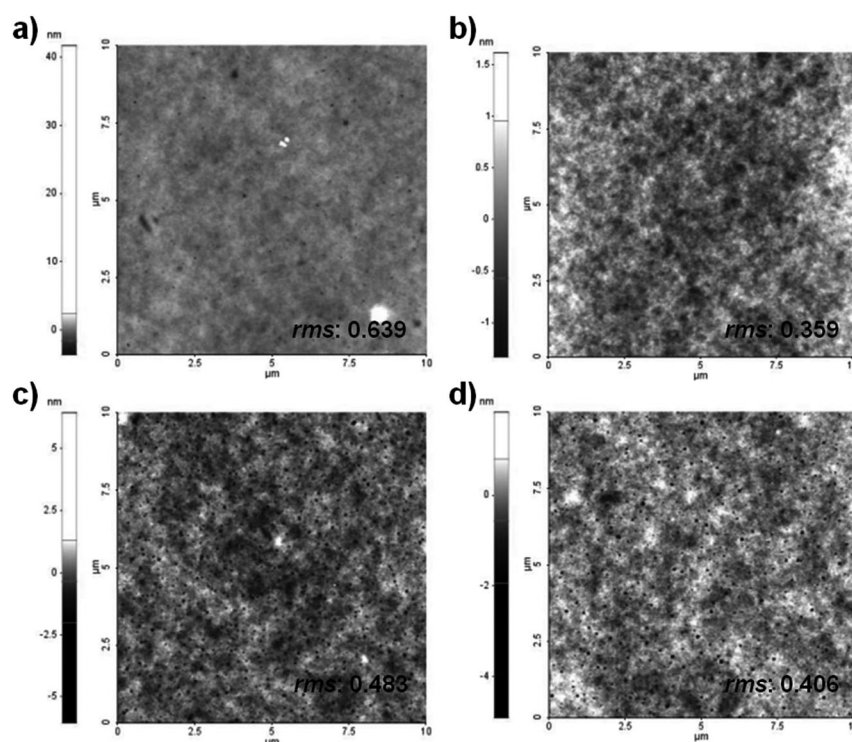


Figure 7. Tapping-mode AFM surface topography of films cast from TIPSAntBT-TPA/PC₇₁BM (1:4) BHF composite without (a) or with (b) treatment with 1% CN, and TIPSAntBT-bisDMFA/PC₇₁BM (1:4) without (c) or with (d) treatment with 1% CN.

0.41, and $V_{oc}=0.85$ V. Compared with films without a TiO_x layer and without either CN treatment or TiO_x insertion, the efficiency was about 1.5 and 3 times greater, respectively.

Devices fabricated with TIPSAntBT-TPA/PC₇₁BM film treated with a CN processing additive and a TiO_x layer also exhibited a PCE of 1.97% (± 0.15), with $J_{sc}=6.07$ mA cm⁻², $FF=0.40$, and $V_{oc}=0.72$ V, namely, about 33% less than that of TIPSAntBT-bisDMFA/PC₇₁BM. These results might be due to the TIPSAntBT-bisDMFA/PC₇₁BM BHF films having a better surface morphology than that of TIPSAntBT-TPA/PC₇₁BM, resulting in a 13% higher root-mean-square (rms) value, as shown in Figure 7. These rougher nanoscale surfaces might be responsible for the more phase-segregated morphology of the TIPSAntBT-bisDMFA/PC₇₁BM BHF films.

Conclusions

We have demonstrated the synthesis and photovoltaic characteristics of two electron-rich anthracene derivatives, 2,6-bis[5,5'-bis(*N,N'*-diphenylamine)-2,2'-bithiophen-5-yl]-9,10-bis-[(triisopropylsilyl)ethynyl]anthracene (TIPSAntBT-TPA) and 2,6-bis(5,5'-bis[4-[bis(9,9-dimethyl-9*H*-fluoren-2-yl)amino]phenyl]-2,2'-bithiophen-5-yl)-9,10-bis-[(triisopropylsilyl)ethynyl]anthracene (TIPSAntBT-bisDMFA), containing triarylamine hole stabilizer, which exhibited a maximum power conversion efficiency of 2.96% in solution-processed anthracene derivative-based small-molecule organic solar cells (SMOSCs). These new materials exhibited superior intramolecular charge transfer from TPA

(or bisDMFA) to anthracene through a π -conjugated bithiophene bridge, leading to a more electron-rich anthracene core. This could facilitate electron transfer into PC₇₁BM, resulting in improved hole-transporting properties. The results obtained from the molecular engineering approaches shown in this study could provide a useful guide for developing new materials for use in solution-processed small-molecule bulk hetero junction solar cells.

Experimental Section

The BHF films were prepared under optimized conditions, according to the following previously reported procedure.^[15] The ITO-coated glass substrate was first cleaned with detergent, ultrasonicated in acetone and isopropyl alcohol, and subsequently dried overnight in an oven. PEDOT:PSS (Heraeus, Clevis P VP. Al 4083) in aqueous solution was spin-cast to

form a film with a thickness of approximately 40 nm. The substrate was dried for 10 min at 140 °C in air and then transferred into a glove box for spin-casting of the photoactive layer. The donor/PC₇₁BM BHF blends, TIPSAntBT-TPA/PC₇₁BM or TIPSAntBT-bisDMFA/PC₇₁BM (weight ratio, 1:4), solutions were prepared in chlorobenzene at a concentration of 30 mg mL⁻¹, then heated to 60 °C overnight, followed by spin-casting on top of the PEDOT layer. The substrate was dried for 10 min at 80 °C in air. Then, the device was evacuated to less than 1.33×10^{-5} Pa and an Al electrode about 100 nm thick was deposited on top. The solar cell efficiencies were characterized under simulated 100 mW cm⁻² AM 1.5G irradiation from a 1000 W Xe arc lamp (Oriol 91193). The light intensity was adjusted by a Si solar cell double-checked with an NREL-calibrated Si solar cell (PV Measurement Inc.). The applied potential and cell current were measured by using a Keithley model 2400 digital source meter. The J - V characteristics of the cell under these conditions were determined by biasing the cell externally and measuring the generated photocurrent. This process was fully automated by using Wavemetrics software. The IPCE spectra for the cells were measured on an IPCE measuring system (PV measurements).

The TiO_x material was prepared according to the following previously reported procedure.^[14] Titanium(IV) isopropoxide (10 mL) was slowly added dropwise to a mixture of 2-methoxyethanol (50 mL) and ethanolamine (5 mL) under argon. Then, the mixed solution was heated to 80 °C for 2 h, followed by heating to 120 °C for 1 h. The two-step heating (80 and 120 °C) was then repeated. The dense TiO_x solution was diluted with isopropanol to prepare the typical TiO_x precursor solution. This precursor solution was spin-cast in air on top of the semiconducting photoactive layer, with thicknesses in the range of 10–20 nm. Subsequently, the films were heated at 80 °C for 10 min in air.

Acknowledgements

This research was supported by the World Class University program funded by the Ministry of Education, Science and Technology through the National Research Foundation of Korea (R31-2011-000-10035-0) and MEST for the Center for Next Generation Dye-Sensitized Solar Cells (no. 2011-0001055).

Keywords: anthracenes • bulk heterojunctions • charge transfer • semiconductor • solar cells

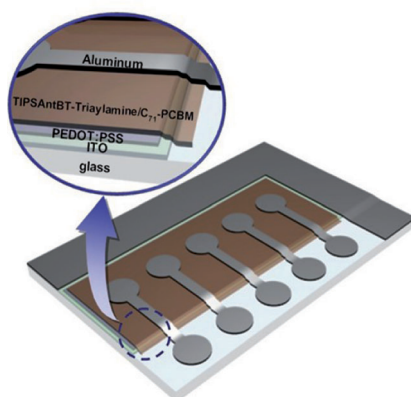
- [1] a) D. Demeter, T. Rousseau, P. Leriche, T. Cauchy, R. Po, J. Roncali, *Adv. Funct. Mater.* **2011**, *21*, 4379–4387; b) B. Walker, C. Kim, T.-Q. Nguyen, *Chem. Mater.* **2011**, *23*, 470–482.
- [2] M. A. Green, K. Emery, Y. Hishikawa, W. Warta, E. D. Dunlop, *Prog. Photovoltaics* **2011**, *19*, 565–572.
- [3] a) S. C. Price, A. C. Stuart, L. Yang, H. Zhou, W. You, *J. Am. Chem. Soc.* **2011**, *133*, 4625–4631; b) H. Zhou, L. Yang, A. C. Stuart, S. C. Price, S. Liu, W. You, *Angew. Chem.* **2011**, *123*, 3051–3054; *Angew. Chem. Int. Ed.* **2011**, *50*, 2995–2998.
- [4] a) S. Roquet, A. Cravino, P. Leriche, O. Alévêque, P. Frère, J. Roncali, *J. Am. Chem. Soc.* **2006**, *128*, 3459–3466; b) A. Cravino, P. Leriche, O. Alévêque, S. Roquet, J. Roncali, *Adv. Mater.* **2006**, *18*, 3033–3037; c) A. B. Tamayo, X. D. Dang, B. Walker, J. Seo, T. Kent, T. Q. Nguyen, *Appl. Phys. Lett.* **2009**, *94*, 103301; d) C. Q. Ma, M. Fonrodona, M. C. Schikora, M. M. Wienk, R. A. J. Janssen, P. Bauele, *Adv. Funct. Mater.* **2008**, *18*, 3323–3331; e) Z. E. Ooi, T. L. Tam, R. Y. C. Shin, Z. K. Chen, T. Kietzke, A. Sellinger, M. Baumgarten, K. Mullen, J. C. deMello, *J. Mater. Chem.* **2008**, *18*, 4619–4622; f) J. Lee, M. H. Yun, J. Kim, J. Y. Kim, C. Yang, *Macromol. Rapid Commun.* **2012**, *33*, 140–145; g) J. Lee, J. Kim, G. Kim, C. Yang, *Tetrahedron* **2010**, *66*, 9440–9444.
- [5] Y. Sun, G. C. Welch, W. L. Leong, C. J. Takacs, G. C. Bazan, A. J. Heeger, *Nat. Mater.* **2012**, *11*, 44–48.
- [6] a) H. M. Ko, H. Choi, S. Paek, K. Kim, K. Song, J. K. Lee, J. Ko, *J. Mater. Chem.* **2011**, *21*, 7248–7253; b) B. S. Jeong, H. Choi, N. Cho, H. M. Ko, W. Lim, K. Song, J. K. Lee, J. Ko, *Sol. Energy Mater. Sol. Cells* **2011**, *95*, 1731–1740; c) S. So, H. Choi, C. Kim, N. Cho, H. M. Ko, J. K. Lee, J. Ko, *Sol. Energy Mater. Sol. Cells* **2011**, *95*, 3433–3441; d) S. So, H. Choi, H. M. Ko, C. Kim, S. Paek, N. Cho, K. Song, J. K. Lee, J. Ko, *Sol. Energy Mater. Sol. Cells* **2012**, *98*, 224–232; e) H. Choi, S. Paek, J. Song, C. Kim, N. Cho, J. Ko, *Chem. Commun.* **2011**, *47*, 5509–5511.
- [7] a) M. M. Payne, S. R. Parkin, J. E. Anthony, C.-C. Kuo, T. N. Jackson, *J. Am. Chem. Soc.* **2005**, *127*, 4986–4987; b) G. Laquindanum, H. E. Katz, A. J. Lovinger, *J. Am. Chem. Soc.* **1998**, *120*, 664–672; c) M. T. Lloyd, A. C. Mayer, S. Subramanian, D. A. Mourey, D. J. Herman, A. V. Bapat, J. E. Anthony, G. G. Malliaras, *J. Am. Chem. Soc.* **2007**, *129*, 9144–9149; d) M. M. Payne, S. A. Odom, S. R. Parkin, J. E. Anthony, *Org. Lett.* **2004**, *6*, 3325–3328.
- [8] D. S. Chung, J. W. Park, J. W. Park, D. Moon, G. H. Kim, H. S. Lee, D. H. Lee, H. K. Shim, S. K. Kwon, C. E. Park, *J. Mater. Chem.* **2010**, *20*, 524–530.
- [9] D. S. Chung, J. W. Park, W. M. Yoon, H. Cha, Y. H. Kim, S. K. Kwon, C. E. Park, *ChemSusChem* **2010**, *3*, 742–748.
- [10] a) J.-H. Park, D. S. Chung, J.-W. Park, T. Ahn, H. Kong, Y. K. Jung, J. Lee, M. H. Yi, C. E. Park, S.-K. Kwon, H.-K. Shim, *Org. Lett.* **2007**, *9*, 2573–2576; b) D. Kim, M.-S. Kang, K. Song, S. O. Kang, J. Ko, *Tetrahedron* **2008**, *64*, 10417–10424; c) W. Li, C. Du, F. Li, Y. Zhou, M. Fahlman, Z. Bo, F. Zhang, *Chem. Mater.* **2009**, *21*, 5327–5334.
- [11] a) J. Pommerehne, H. Vestweber, W. Guss, R. F. Mahrt, H. Bassler, M. Porsch, J. Daub, *Adv. Mater.* **1995**, *7*, 551–554; b) Z. Chen, M. G. Debije, T. Debaerdemaeker, P. Osswald, F. Würthner, *ChemPhysChem* **2004**, *5*, 137–140.
- [12] M. C. Scharber, D. Mühlbacher, M. Koppe, P. Denk, C. Waldauf, A. J. Heeger, C. J. Brabec, *Adv. Mater.* **2006**, *18*, 789–794.
- [13] V. D. Mihailetschi, H. Xie, B. Boer, L. J. A. Koster, P. W. M. Blom, *Adv. Funct. Mater.* **2006**, *16*, 699–708.
- [14] K. Lee, J. Y. Kim, S. H. Park, S. H. Kim, S. Cho, A. J. Heeger, *Adv. Mater.* **2007**, *19*, 2445–2449.
- [15] J. K. Lee, W. L. Ma, C. J. Brabec, J. Yuen, J. S. Moo, J. Y. Kim, K. Lee, G. C. Bazan, A. J. Heeger, *J. Am. Chem. Soc.* **2008**, *130*, 3619–3623.

Received: April 5, 2012

Published online on ■ ■ ■, 0000

FULL PAPERS

Digging deeper: New electron-rich anthracene derivatives containing a triarylamine hole stabilizer, TIPSAntBT-TPA and TIPSAntBT-bisDMFA, exhibit superior intramolecular charge-transfer performance, resulting in a boost in hole-transporting properties (see picture).



*H. Choi, H. M. Ko, N. Cho, K. Song,
J. K. Lee,* J. Ko**



**Electron-Rich Anthracene
Semiconductors Containing
Triarylamine for Solution-Processed
Small-Molecule Organic Solar Cells**

